

Chapter 4 Results and Discussions

4.1 Introduction

The radiation produced by the 600 joules small plasma focus device is investigated experimentally. The discharge current and the voltage are interpreted together with the radiation output in order to determine good operating conditions. Argon gas is used and the operating pressure is varied from few mbar down to 10^{-3} mbar to obtain suitable operating pressure for good focusing discharge. X-ray emission and the EUV emission from the plasma are measured simultaneously with the discharge current and the voltage. Additionally, the ion beams produced from the plasma are also investigated.

4.2 Plasma Focus Discharge at Low Operating Pressure

The plasma focus tube used in the current project is designed to allow operation at low pressure. Nonetheless experiments are carried out in a broad range of operating pressure from several mbar to 10^{-3} mbar to determine a suitable range of operating pressure. Ten or more shots are run for each operating pressure under the investigation. Argon gas is flown continuously into the chamber to reduce the impurity gases inside the tube and maintain the operating pressure simultaneously.

The appearance of the distinct and sharp voltage spike and current dip in the voltage and current signals respectively are used as the indicator for successful operation of the dense plasma focus device. The voltage spike and current dip are the consequence of the rapid change in plasma impedance during pinching. The increase in the plasma

impedance is being attributed to fast changing plasma inductance and growth in anomalous resistance.

Upon formation of the plasma column, radiations are emitted based on the plasma characteristics. In argon discharge, visible light, X-ray, EUV could be produced with their yield depends on the condition of the pinched plasma. For the current setup, in a narrow pressure regime of 9.0×10^{-3} mbar to 2.2×10^{-2} mbar, focusing action has been observed with good reproducibility, where X-ray, EUV and ion beam emission are also observed to be significant.

Figure 4.1 shows a set of signals obtained at 3.0×10^{-2} mbar. At this pressure and all other pressures out of the pressure regime that has been indentified above, no focusing has been observed. These are discharges without focusing. In these discharges, it is noticed that the voltage and the current signal resemble the light damping oscillations, little amount of ultra-soft emission has been registered occasionally, but no EUV has been observed. With reference to the XRD signal in Figure 4.1, the emission is likely to be between $18 \text{ \AA} - 60 \text{ \AA}$, emitted from the current sheath during the axial phase.

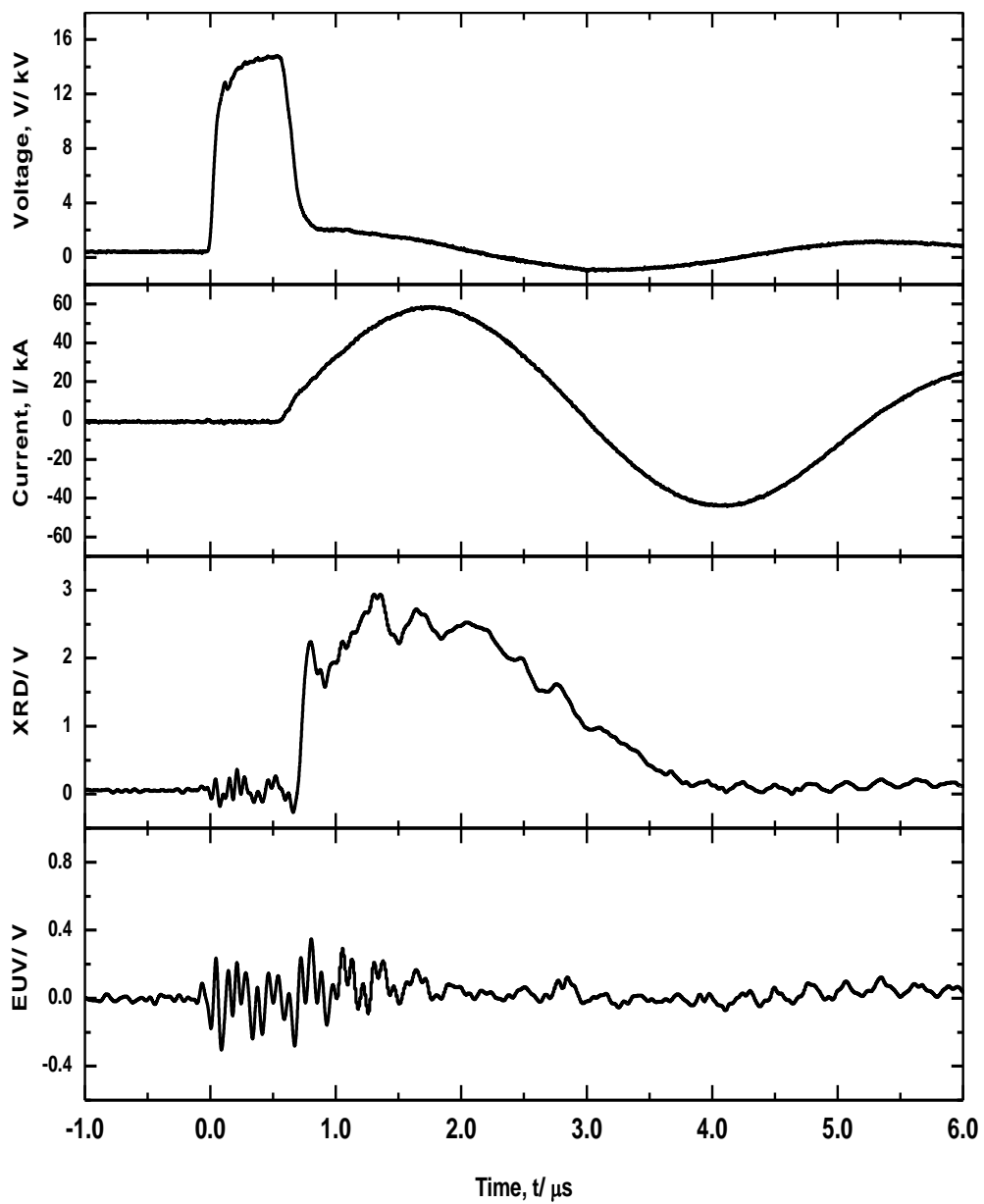


Figure 4.1 Electrical, XRD and EUV signals obtained for non-focusing argon discharge at 3.0×10^{-2} mbar, 18 kV.

Focusing discharge occurs predominantly in the pressure range of 2.2×10^{-2} mbar to 9.0×10^{-3} mbar. A typical set of signals is shown in Figure 4.2, obtained at 1.8×10^{-2} mbar. In the figure, we notice that the voltage across the electrodes breakdowns at $t = 0.94 \mu\text{s}$, after which the current rises rapidly and reaches the peak of 70 kA in a duration of 990 ns. The axial acceleration phase last about 700 ns when the current sheath enters the radial compression phase at the open end of the electrodes. The voltage spike and the current dip registered at $t = 1.64 \mu\text{s}$ are associated with the plasma focus formation.

In the present system, focusing is usually obtained before the discharge current reaches its maximum. In most of the shots, it occurs when current is about 70 % to 90 % of the peak current. The amplitude of the voltage spike registered is about 4 kV to 13 kV. Emission of EUV and X-ray are observed for all the focusing shots. Both EUV and XRD signals rise together with the changes in current and voltage signals. For higher operating pressures, the EUV and X-ray emission peaks are observed later than the voltage spike. However as the operating pressure is decreased, the EUV emission peak is slightly before the voltage spike. This observation indicates that a significant amount of EUV emission is emitted from the hot plasma formed in the pinch plasma slightly before the maximum compression. For the case of discharge shown in Figure 4.2, the EUV and X-ray peaks are registered at about 140 ns after the voltage spike. The full width at half maximum (FWHM) of the EUV and the XRD time profiles are about 160 ns and 270 ns, respectively. The results show that both the EUV and the ultra-soft radiation are emitted after the formation of the pinched plasma or during its decay.

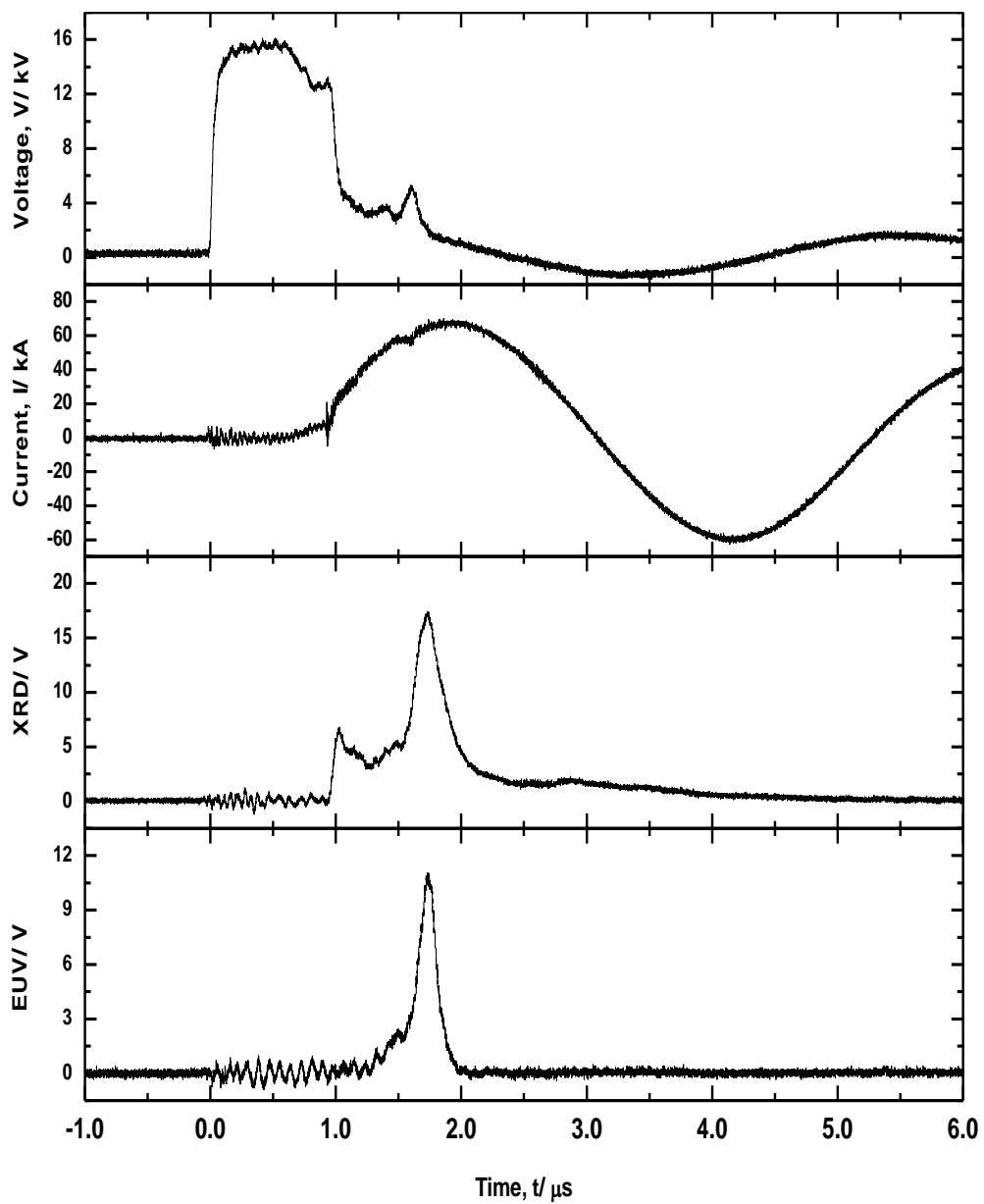


Figure 4.2 Electrical, XRD and EUV signals obtained for argon discharge at 1.8×10^{-2} mbar, 18 kV.

When the operating pressure is lowered, the delay time for breakdown of voltage across the electrodes is also longer. One of the results is shown in Figure 4.3, where the operating pressure is 1.5×10^{-2} mbar and the delay before the voltage breakdowns is 1.28 μ s, compared to 0.97 μ s in Figure 4.2. The discharge voltage is at 18.0 kV for all operating pressures. It is to be noted that the current sheath accelerated more in this pressure and the axial phase last only 680 ns. Generally, higher voltage spike is observed at lower operating pressure, indicating a more severe pinching. In this operating pressure, the EUV and X-ray signals last longer with FWHM of 340 ns and 430 ns, respectively. This confirms that the radiations are emitted from the decaying plasma, lasting longer for hotter plasma.

In general, plasma focus is observed consistently in about 80 % of the shots in the pressure range from 9.0×10^{-3} mbar to 2.2×10^{-2} mbar. A statistical count is presented in Figure 4.4 by analyzing the data obtained for argon pressure from 8.0×10^{-3} mbar to 2.2×10^{-2} mbar, performing fifteen discharges at each pressure. A discharge is further categorized into single focus or multiple foci by referring to the voltage signals registered: single voltage spike or multiples voltage spikes. The discharge tends to form multiple pinching at lower pressure. At pressure lower than 1.0×10^{-2} mbar, probability of getting focusing action is reduced. The results show that less than 70% of the argon discharges have good focus at 9.0×10^{-3} mbar and reduced further to less than 30 % at 8.0×10^{-3} mbar. The discharge in the range of 9.0×10^{-3} mbar to 2.2×10^{-2} mbar has higher probability to obtain the focus with single pinch but focusing is mild, as indicated by the low voltage spike and unclear current dip. In this case, the emission profiles are low. Thus the best condition for good focusing discharge is identified to be in the range of 1.0×10^{-2} mbar to 1.8×10^{-2} mbar although most of the shots exhibit multiple pinches. The total emission is also higher in this

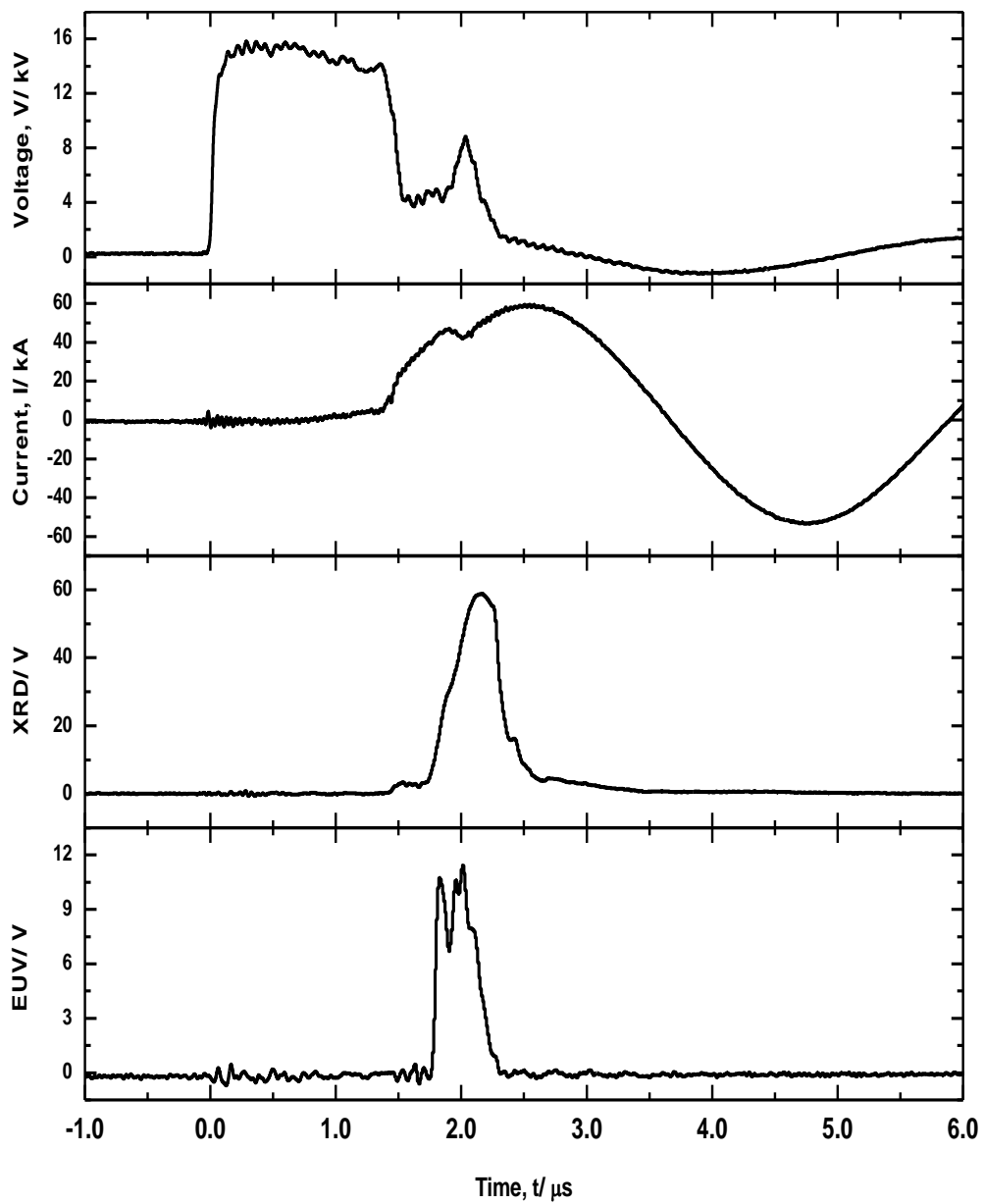


Figure 4.3 Electrical, XRD and EUV signals obtained for argon discharge at 1.5×10^{-2} mbar, 18 kV.

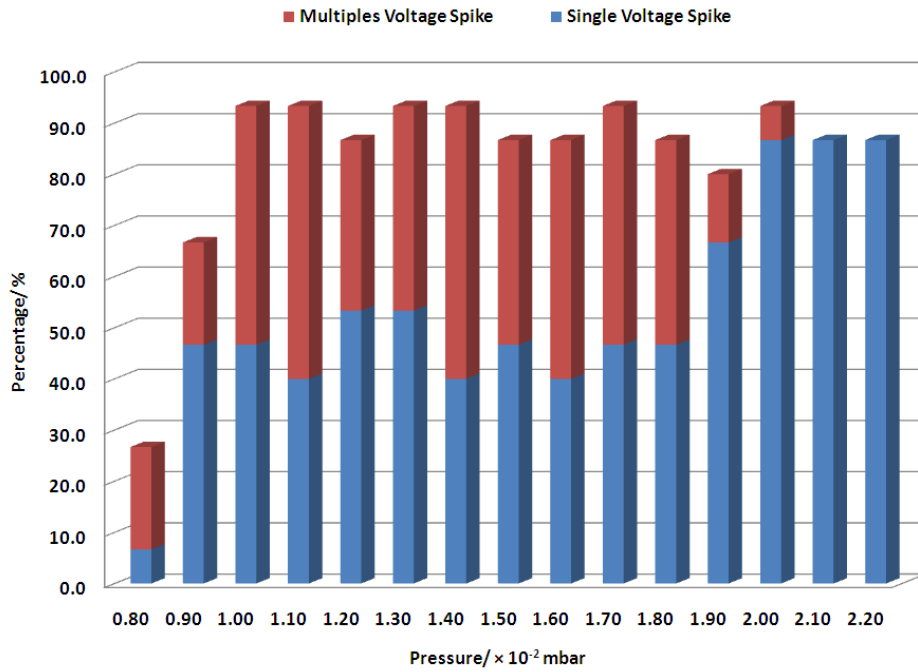


Figure 4.4 Percentage of the discharges producing plasma pinch from the 600 joules small plasma focus device.

pressure regime.

The breakdown of the voltage across the electrode gap correlates strongly to the profile of the electrodes at the backwall and the density of the ambient gas. Thus the voltage breakdown time relates closely to the operating pressure as shown in the experiments. At the charging voltage of 18 kV and the gap between the anode and the knife edge cathode at the backwall of 10 mm, breakdown time versus operating pressure is plotted in Figure 4.5.

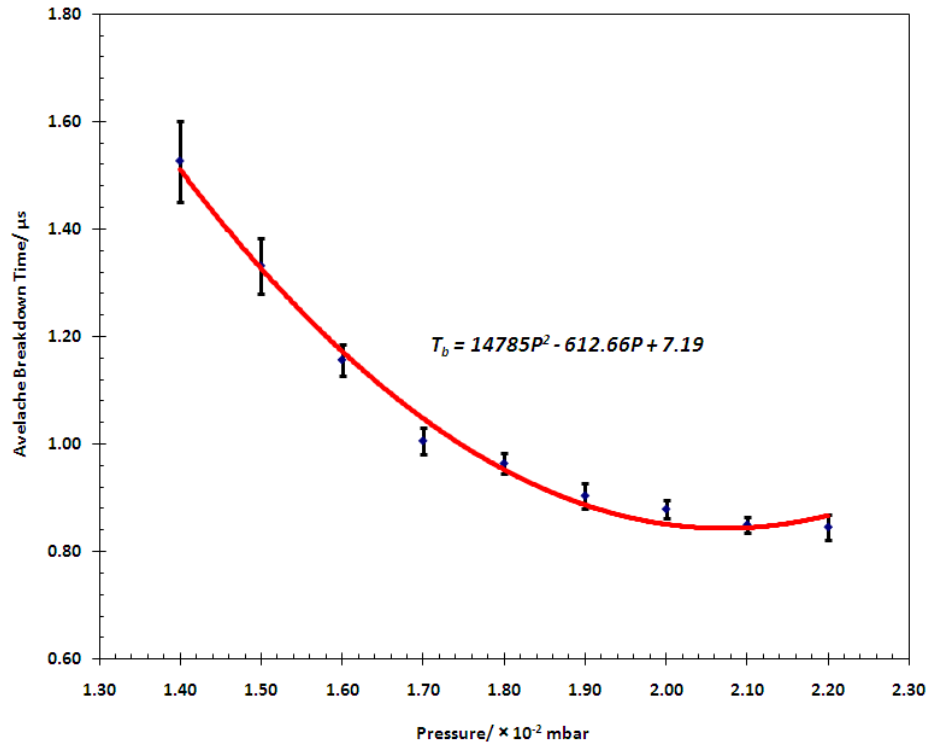


Figure 4.5 Breakdown time at different argon pressures.

$T_b = 14785P^2 - 612.66P + 7.19$ represents the relation between the breakdown time T_b (μs) and the operating pressure P (mbar).

In the present system, the discharge current has a rise time of 950 ns. This matches well with the electrode geometry by operating in the low pressure regime. In order to estimate the rundown time in the axial acceleration phase, the duration from the time of the breakdown to the formation of the plasma focus at the open end of the anode is measured. The average velocity of the current sheath is thus calculated. The results vary from 8.5 ± 0.4 cm/ μs to 12.2 ± 0.8 cm/ μs . These values conform to many other experimental observations. It is often reported that an average velocity of around 8 cm/ μs to 12 cm/ μs usually leads to good plasma focus [Lee et al. (1988), Yap et al. (2009)].

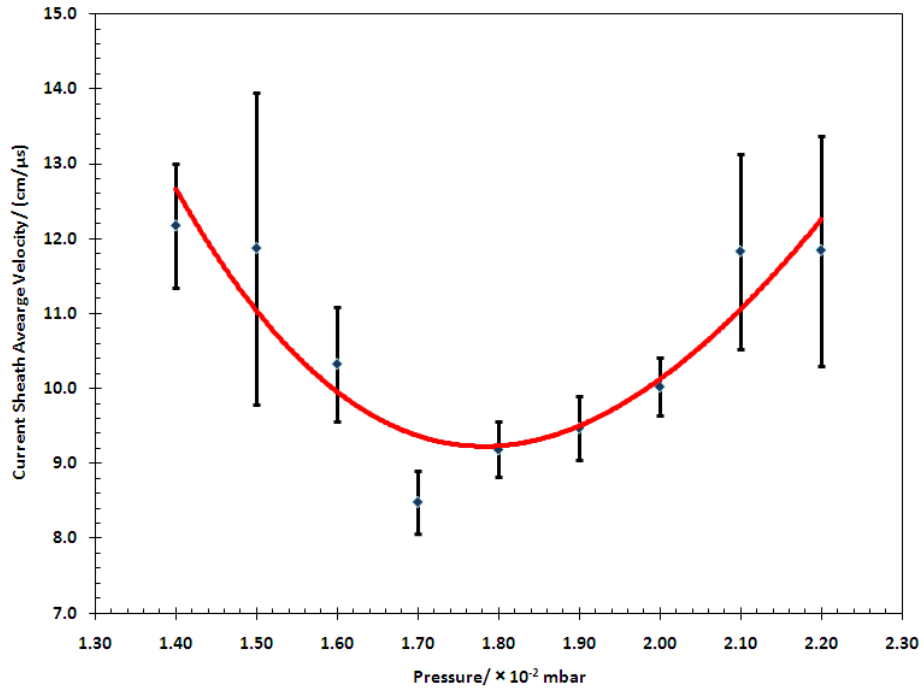


Figure 4.6 The average velocity of the current sheath at different argon pressure.

Figure 4.6 shows the average velocity of the current sheath at different argon pressure. The average velocity of the current sheath decreases when the operating pressure reduces from 2.2×10^{-2} mbar to 1.8×10^{-2} mbar and rise back for lower pressures. The lowest average velocity obtained is 8.5 ± 0.4 cm/ μ s at 1.7×10^{-2} mbar. The lower average velocity indicates a higher rate of mass shedding, where the current sheath sweeps up more gas particles encountered thus carries more mass in the axial acceleration phase. The large standard deviation of the average velocity observed at some pressures is due to the shot to shot variation.

The drive parameter, S given by $I_o/ap^{1/2}$ and the parameter D given by I_o/a (where the I_o , a , p are peak current, anode radius and operating pressure, respectively) of our setup are 1203 (kA/cm)/torr $^{1/2}$ and 147 kA/cm, respectively. The drive parameter S and D for many plasma focus devices fall in a range of 89 ± 8 (kA/cm)/torr $^{1/2}$ and 150 kA/cm to 220 kA/cm, respectively [Lee et al. (1996), Lee et al. (1998)]. The S value

corresponds to an axial speed of just less than 10 cm/ μ s. This value is about the same as the average velocity measured in our experiments. Thus, one might expect the drive parameter, S and parameter D fall in the same range. However, the drive parameter, S obtained for our system is significantly higher, 8-folds, compared to other devices.

It is important to note that the drive parameter, S depends linearly on the parameter D and half power of the pressure p . As our device has been designed to work at a much lower pressure, the drive parameter obtained is thus much higher.

4.3 Emission Characteristics of the Plasma Focus Discharge

EUV emission in the range of 110 Å - 180 Å from the 600 joules small plasma focus are detected by using a fast filtered photodiode, SXUV5A with integrated thin film filters of 100 nm Si/ 200 nm Zr. Ultra-soft X-radiation measured by the X-ray Diode (XRD) that has a spectral sensitivity windows in the range of 6Å to 600 Å. The setups for these detectors have been described in Chapter 3 (Section 3.3.3 and Section 3.3.4). In this experiment, about twenty shots are carried out at each operating pressure, while the gas is refreshed every 5 shots to ensure minimal impurity inside the chamber.

In this series of experiment, radiations are measured together with the discharge voltage and current for the operating pressures of 9.0×10^{-3} mbar to 2.2×10^{-2} mbar. At higher operating pressure, the radiation yield is relatively small. Typical signals are shown in Figure 4.7 for discharge pressure of 2.0×10^{-2} mbar. Radiation increases when the operating pressure is reduced. Maximum EUV radiation is obtained when the operating pressure is 1.6×10^{-2} mbar. A set of signals is shown in Figure 4.8. Ultra-soft X-radiations are observed to be highest at 1.4×10^{-2} mbar, with some EUV radiation (Figure 4.9).

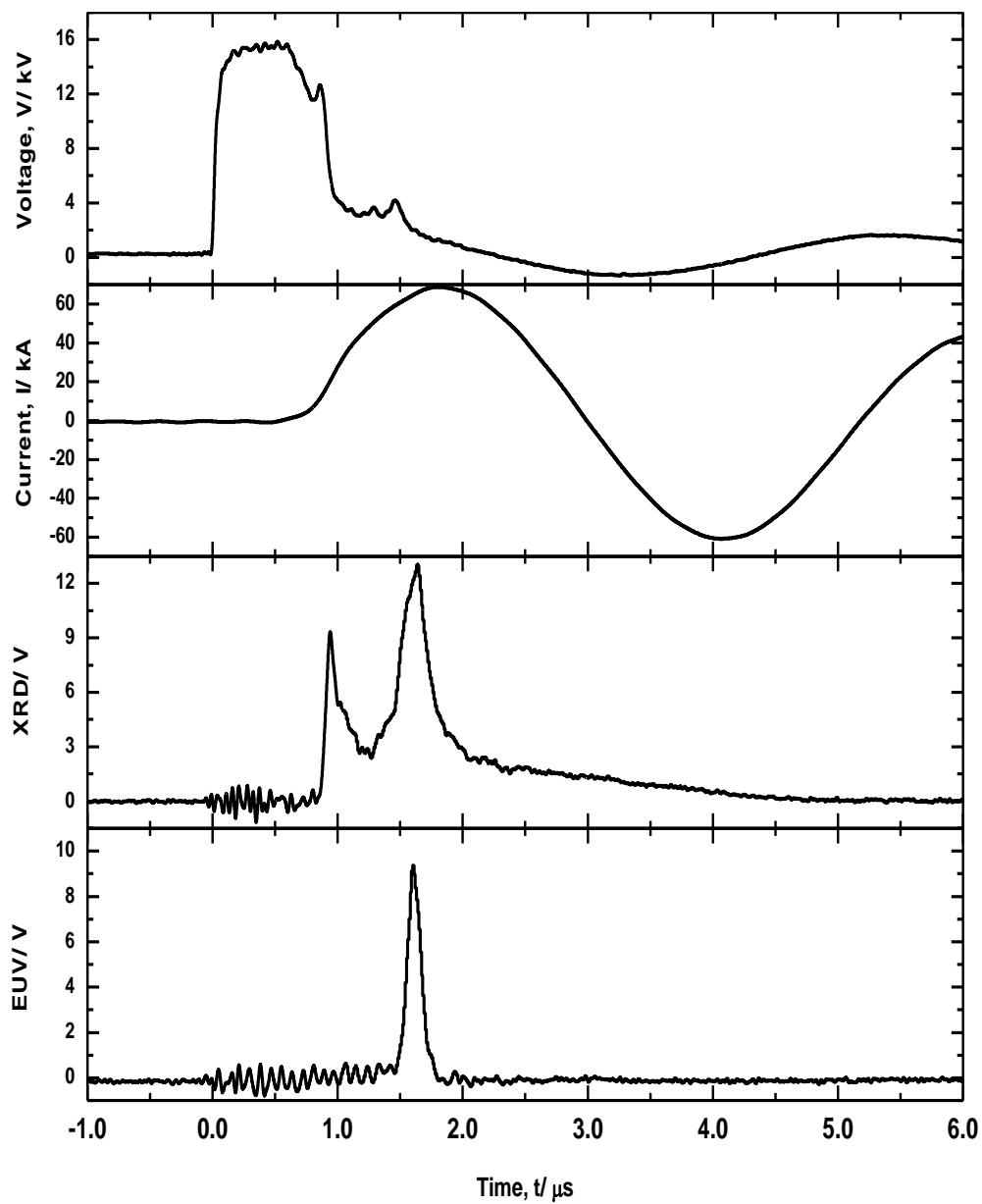


Figure 4.7 Electrical, XRD and EUV signals obtained for argon discharge at 2.0×10^{-2} mbar, 18 kV.

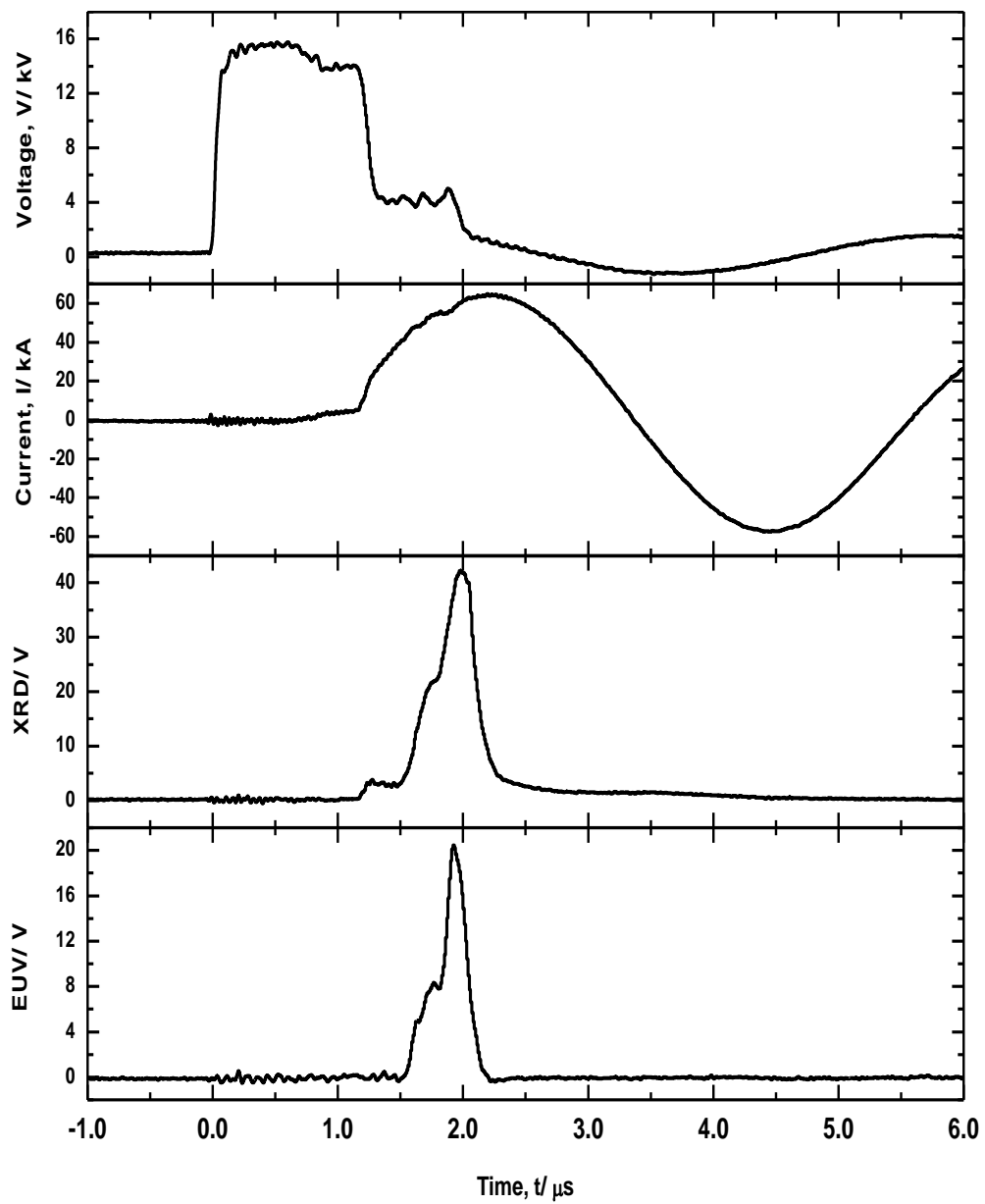


Figure 4.8 Electrical, XRD and EUV signals obtained for argon discharge at 1.6×10^{-2} mbar, 18 kV.

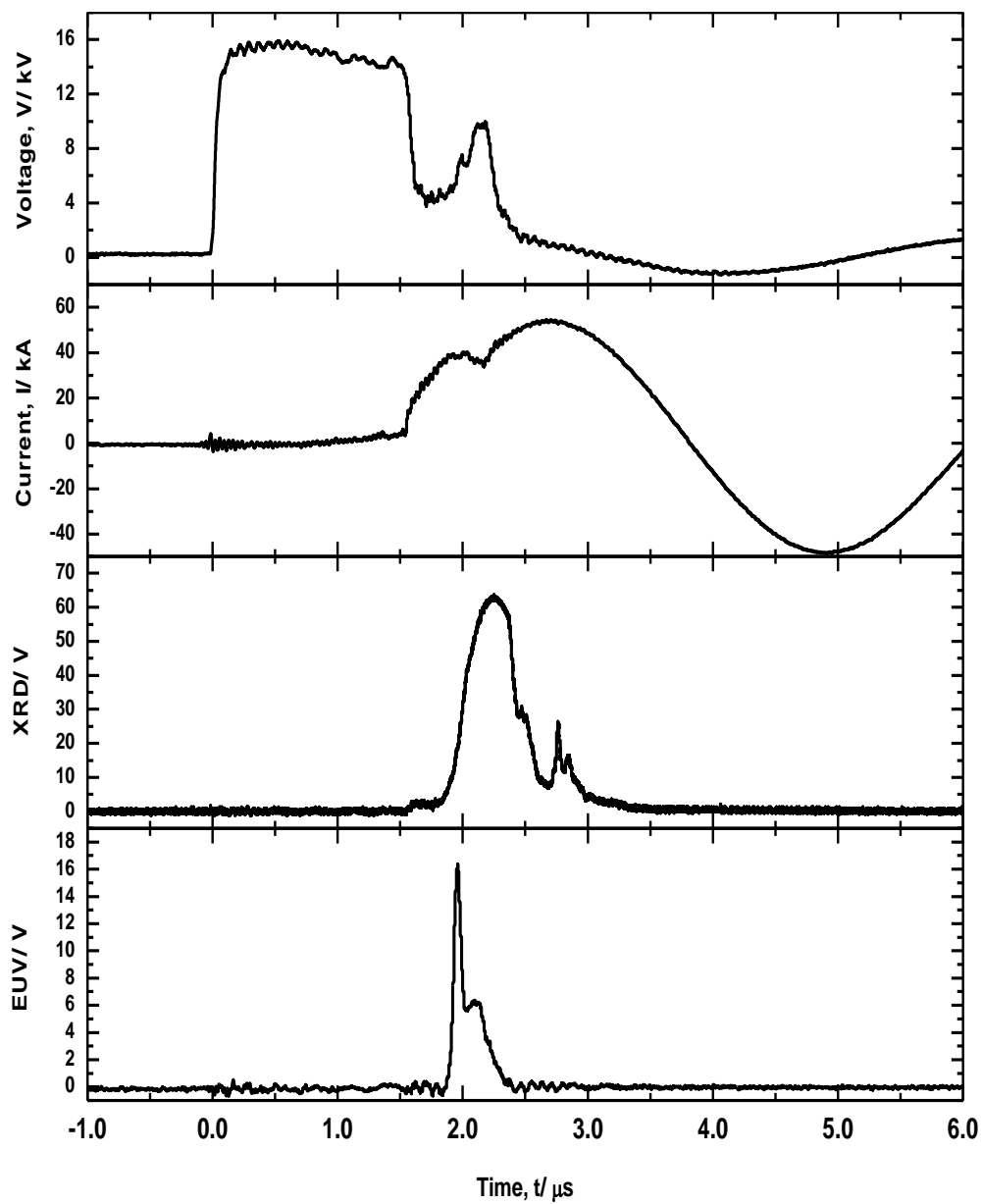


Figure 4.9 Electrical, XRD and EUV signals obtained for argon discharge at 1.4×10^{-2} mbar, 18 kV.

A set of signals that is obtained at 2.0×10^{-2} mbar is shown in Figure 4.7. The amplitude of the current signal measured is about 69 kA. The first peak of the XRD signal is registered during the voltage breakdown across the electrodes. This emission is likely to be due to the electron bombardments of the electrodes. Softer emission including the EUV is not observed here. The plasma focus is formed at around 1.6 μ s where various emissions are observed. A small voltage spike and insignificant current dip are observed. A sharp pulse of EUV is registered, but the total EUV radiation is much less compared to those obtained at lower pressures. The EUV signal has a FWHM of 140 ns and its rise time is around 130 ns. The XRD signal consists of ultra-soft X-radiation and has a FWHM of 170 ns and a much slower rise of around 270 ns.

It is generally observed that when the operating pressure is in the range of 1.6×10^{-2} mbar to 2.2×10^{-2} mbar, small voltage spike and insignificant current dip are obtained. These indicate a mild focus. Figure 4.8 shows a set of signals obtained at 1.6×10^{-2} mbar. Both signals registered by the XRD and EUV detectors are large. The peak of EUV and XRD signals are 20.5 V and 42.2 V compared to 9.4 V and 13.0 V that are shown in Figure 4.7 for higher operating pressures.

At lower pressure, more than one voltage spike and current dip are often observed (Figure 4.9). In these cases, two or more compression of the plasma have occurred thus corresponding pulses of radiations of ultra-soft X-radiation and EUV are registered. The peaks of the XRD and EUV signals can be correlated to the voltage spikes. The ultra-soft X-radiation obtained in this pressure regime is the highest compared to others. The peak value is usually 50 V to 65 V. A second pulse is also registered by the XRD detector at 700 ns after the voltage spike. It usually lasts about

40 ns to 100 ns and is associated with the vaporized copper jet emitted from the inside or the rim of the anode.

The emission from the plasma is correlated to the plasma temperature. A strong compression produces a high temperature plasma focus. This has been observed where the ultra-soft X-radiations emissions are getting stronger at lower operating pressures, indicating a stronger compression of the plasma. However, the highest EUV emissions have been observed at 1.6×10^{-2} mbar where the plasma temperature is just sufficient for EUV emissions in this series of experiment.

The Coronal Equilibrium model (CE model) is used here to predict the population density of the argon plasma at specific temperature. This CE model assumes that electrons are in thermal equilibrium while other parameters such as ion temperature, pressure and various ionization states of ions change slowly. Distribution of the electrons velocities follows Maxwellian distribution function. From the atomic database spectr-W3 [<http://spectr-w3.snz.ru/>] for plasma spectroscopy, dominating argon species that are responsible for the EUV emission are *Ar-VII*, *Ar-VIII*, *Ar-IX*, *Ar-X*, *Ar-XI* and *Ar-XII* (Table 4.1).

The expression for CE model is:

$$\frac{N_{i+1}}{N_i} = \frac{1.27 \times 10^8}{\chi_i^2} \left(\frac{kT_e}{\chi_i} \right)^{3/4} \exp\left(-\frac{\chi_i}{kT_e} \right) \quad (4.1)$$

where N_i , χ_i , k , and T_e are the ionic species density of i -th ionized state, ionization potential of i -th ionized state, Boltzmann constant, and electron temperature,

respectively. This expression is used to find the population density ratio of ionic species for argon plasma for electron temperature of 10 eV to 120 eV (Figure 4.10). As electron temperature of the argon plasma rises from 15 eV to 100 eV, the dominating species of argon plasma are the *Ar-VII*, *Ar-VIII*, *Ar-IX*, *Ar-X* and *Ar-XI*. These species emit intense spectral line emissions at wavelength at or near to 13.5 nm (Table 4.1).

On the other hand, plasma continuum emission peak at 13.5 nm corresponds to the temperature of around 46 eV. EUV emission that contributed by the line emission and continuum emission, it is believed that the EUV emission obtained in this experiment is mainly contributed by *Ar-VII* and *Ar-VIII*.

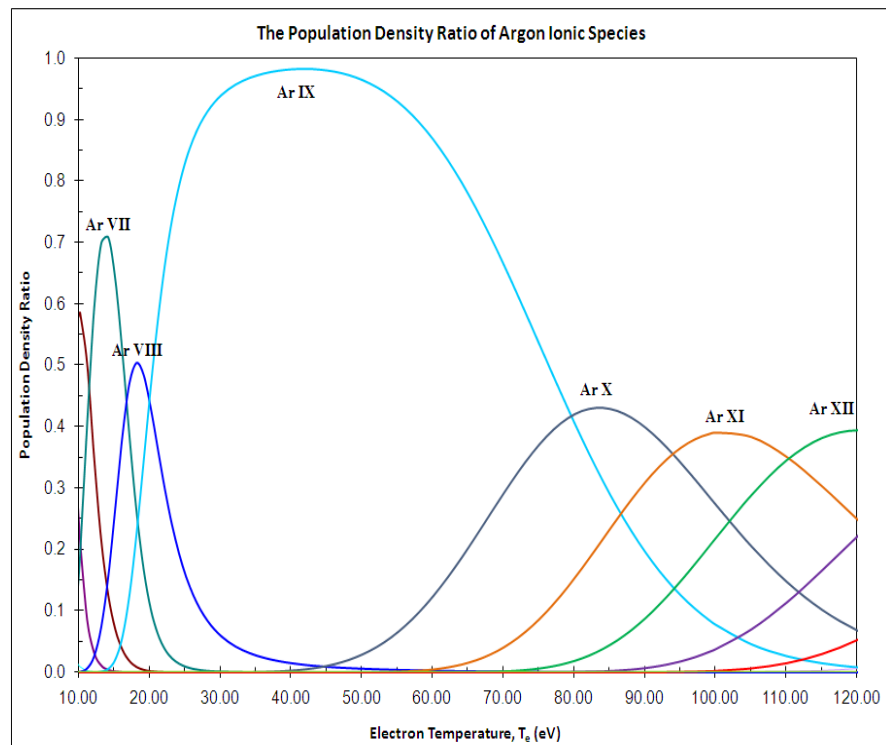


Figure 4.10 Population density ratios of argon ionic species as a function of electron temperature based on the Coronal Equilibrium Model (CE Model).

Table 4.1 Argon ions species with the corresponding characteristics line radiation.

[Source: <http://spectr-w3.snz.ru/>]

Argon Ions	Wavelengths (nm)
Ar-VII (Ar ⁶⁺)	12.0, 12.4 - 12.5, 13.0, 13.2, 13.4, 13.6 - 13.7 , 14.2 - 14.3, 15.1, 16.3, 16.8, 17.5 - 17.6
Ar-VIII (Ar ⁷⁺)	12.0, 12.2 - 12.3, 12.7 - 12.8, 13.5, 13.7 - 14.0 , 14.8 - 15.0, 15.2, 15.8, 17.9 - 18.0, 18.4
Ar-IX (Ar ⁸⁺)	15.7, 16.2
Ar-X (Ar ⁹⁺)	16.5, 17.0
Ar-XI (Ar ¹⁰⁺)	13.3, 13.5 , 15.1, 16.4, 18.1, 18.4 - 18.7
Ar-XII (Ar ¹¹⁺)	12.8, 13.0, 13.2 - 13.3, 13.6 - 13.8 , 15.4, 15.8, 16.0, 16.2 - 16.4, 16.9 - 17.0, 17.3, 17.5 - 17.6, 17.8, 18.4 - 18.5

To conclude the observation in this section, soft X-ray and the EUV emission are significant only in a narrow range of operating pressures. Moreover the amplitude of the soft X-ray and the EUV emission are very sensitive function to the pressure change within this range. Stronger pinched plasma exists at lower operating pressure and is believed to have higher temperature where emission is more towards shorter wavelength. This is observed as stronger XRD signal but weaker EUV signal. At higher pressure, the EUV emission peak is observed later than the voltage spike when suitable condition or plasma temperature is met. In such condition, dominating species are the *Ar-VII* and *Ar-VIII* which produce the EUV emission.

4.3.1 EUV Energy

Under selected conditions, EUV emissions are significantly obtained from the discharge. The total energy due to the EUV emission is calculated here. First, we integrate the EUV signal to obtain the total yield per discharge. Then by assuming the pinched plasma as a point radiation source, the total EUV photon energy emitted can be obtained. This calculation includes all the photons detected which is in the range of 11 nm - 18 nm.

The time-resolved EUV signal registered for the experiment has been plotted in the unit of volts, $V(t)$. The charge, Q generated by the EUV photons in the photodiode per pulse is expressed as

$$Q = \int I(t)dt \quad \text{Coulombs} \quad (4.2)$$

Base on Ohm's Law, $I = V/R$, where I is the current flowing in the detection circuit and V is the voltage across the load resistor, R . In this case, the load resistor is the impedance matching resistor on the oscilloscope with value of 51 Ω . Thus, Equation 4.2 can be expressed as

$$Q = \frac{1}{R} \int V(t)dt \quad \text{Coulombs} \quad (4.3)$$

Based on the total charge measured due to the EUV emission and the sensitivity of the detector, the total energy can be calculated. Here E_p represents the EUV energy measured per discharge can be expressed in Equation 4.4.

$$E_p = \frac{1}{R \cdot S} \int V(t) dt \quad \text{Joules} \quad (4.4)$$

where S is the sensitivity of the EUV detector or the responsivity of the detector which define the ratio of the generated photocurrent to the incident radiation power in the unit of A/W . The responsivity for SXUV is shown in Figure 3.9. The value of S corresponds to photon of 13.5 nm is 0.194 A/W .

Finally, the total EUV energy obtained in 4π can be calculated:

$$E = \frac{\int V(t) dt}{R \cdot S} \cdot \frac{4\pi d^2}{A} \quad \text{Joules} \quad (4.5)$$

with d as the distance between the EUV source to the detector, which is 550 mm and A is the effective detection area of the detector, which is 5 mm².

Figure 4.11 summaries the total EUV energy obtained for discharges of 1.4×10^{-2} mbar to 2.2×10^{-2} mbar. Each data point in the curve represents the averaged value of ten shots. The average total EUV energy is found to vary from 7.77 ± 1.69 mJ to 275.42 ± 23.56 mJ. In general, average total EUV energy is increasing with decreasing operating pressure from 2.2×10^{-2} mbar to nearly 1.6×10^{-2} mbar. Below 1.5×10^{-2} mbar the EUV energy drops. Hence, the optimum EUV energy output of 275 ± 23.56 mJ is estimated at about 1.6×10^{-2} mbar. In Figure 4.11, the large standard deviation of the EUV emission is due to the shot to shot fluctuation which is common in the plasma focus device. If the input energy of the system is considered, the total EUV energy produced corresponds to a conversion efficiency of about 0.0013 % to 0.046 %.

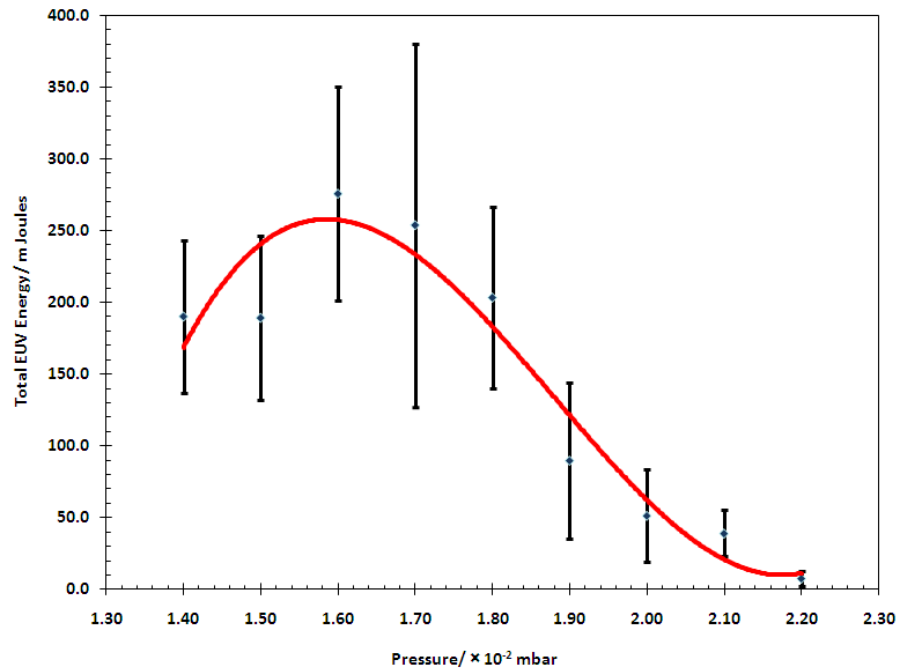


Figure 4.11 Variation of the average total EUV energy at argon pressure of 1.4×10^{-2} mbar to 2.2×10^{-2} mbar. The optimum pressure that emitted highest EUV radiation occurred at about 1.6×10^{-2} mbar.

Emission of EUV is found to depend on the operating pressure of the discharge. Thus, it is believed that the dynamics of the current sheath before the formation of the plasma focused may affect the condition of the plasma and its emissions. The current sheath velocity of discharges at various pressures are plotted together with the average EUV energy obtained to show the possible correlation (Figure 4.12). At the pressure where optimum EUV energy is registered, current sheath average velocity is about $10 \text{ cm}/\mu\text{s}$.

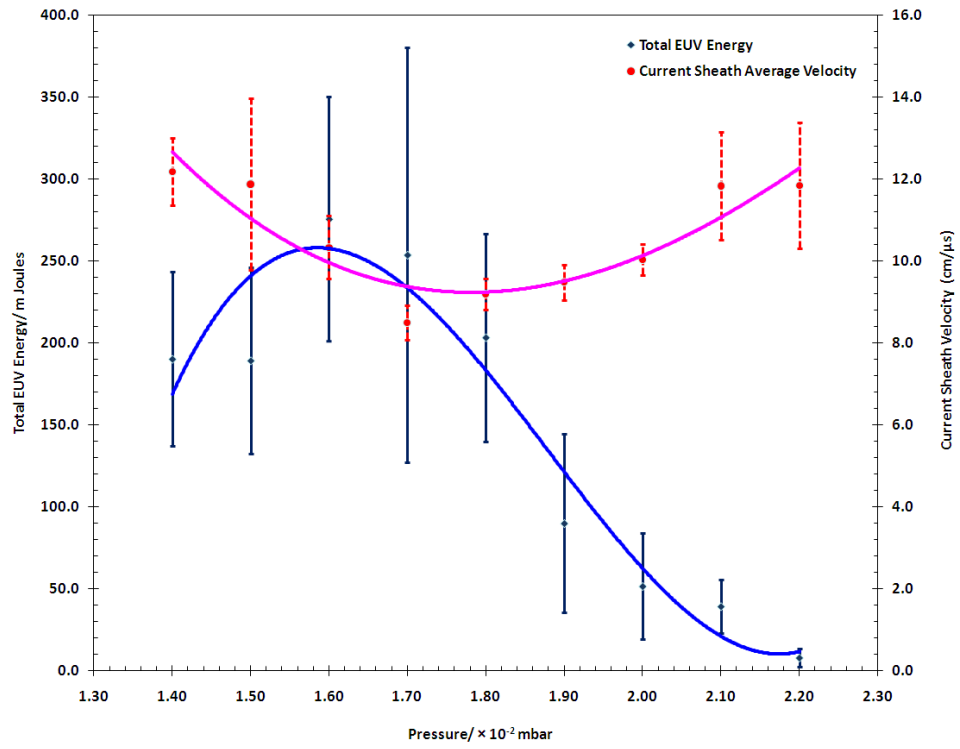


Figure 4.12 Variation of the average total EUV energy and the corresponding of current sheath average velocity at argon pressure of 1.4×10^{-2} mbar to 2.2×10^{-2} mbar.

4.3.2 Ion Beam Energy

The plasma focus discharge also produces ion beam and electron beam. These particle beam emissions are usually correlated to the instability in the plasma. The investigation of ion beam is carried out here to give better understanding of the plasma developed in the discharge. Characteristics of the ion beam will also be studied. Two biased ion collectors are employed here to investigate the characteristics of the ion emissions. They are placed at the end on direction, one at 70 cm from the anode, the other at 140 cm. This arrangement allows us to employ the Time-of-Flight (TOF) technique to determine the argon beam energy.

In this series of experiments, the ion beam produced by the argon discharge is investigated. Time-resolved measurement of the argon beam is achieved by employed the TOF technique, which has been discussed in section 3.3.5. By analyzing the time-resolved signals at two different distances, ion beams as well as the photoemission of the discharge can be determined. Ion beam energies are also calculated by determining the corresponding peaks of the ion beams.

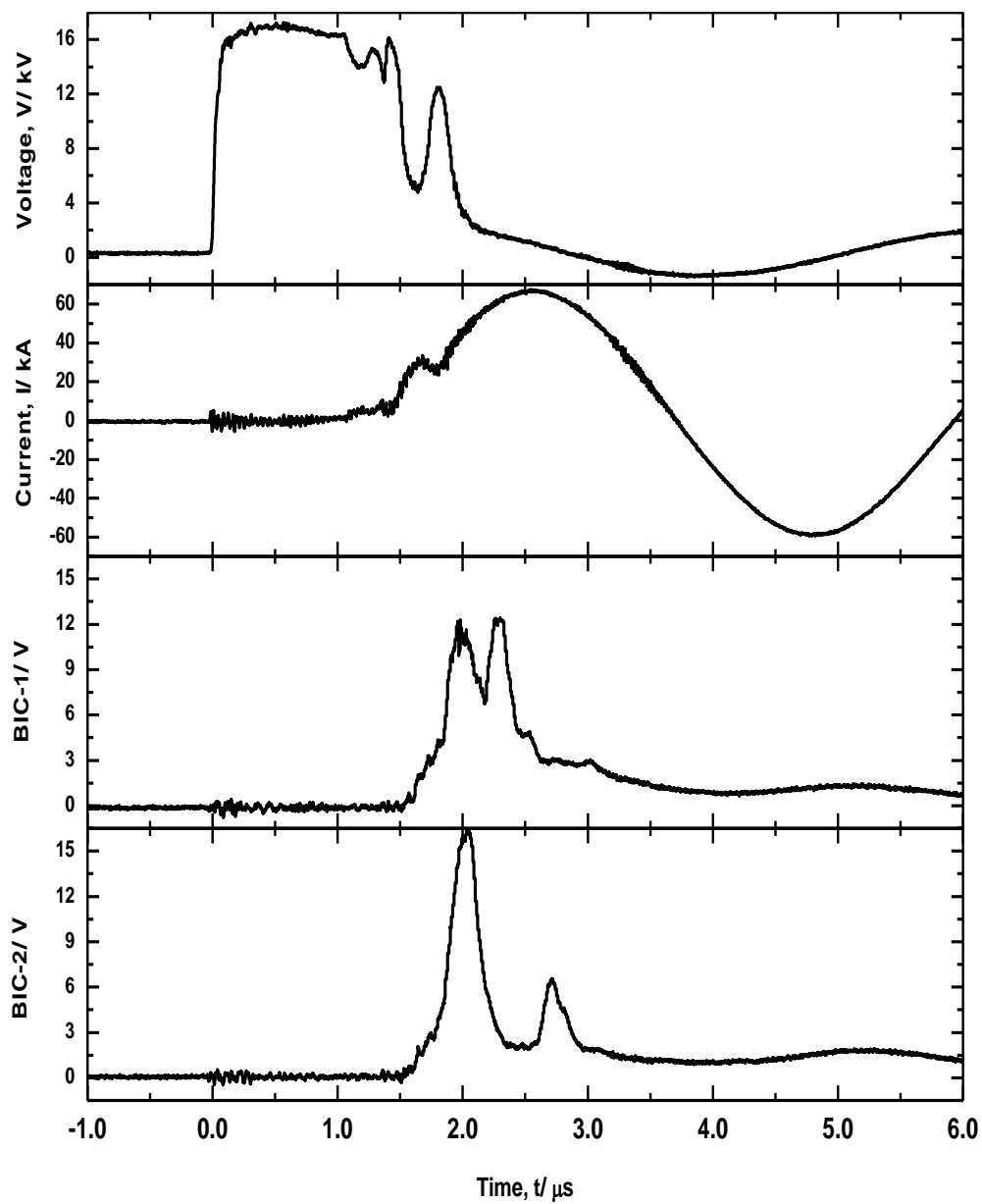


Figure 4.13 Typical electrical and biased ion collector signals obtained for the argon discharge at 9.0×10^{-3} mbar, 18 kV.

The measurements are carried out for the range of pressure of 8.0×10^{-3} mbar to 2.2×10^{-2} mbar. The time resolved signals obtained by the two biased ion collectors clearly show that both photoemission and ion beam signals are detected. Figure 4.13 shows the typical electrical signals and significant ion beam signals for argon discharge that is obtained at 9.0×10^{-3} mbar. The first peaks of both ion collector signals occurred at about the same time are due to photoemissions. The second peaks correspond to the argon beams. The peak values of the argon beam obtained at different pressures are analyzed and compared in Figure 4.14.

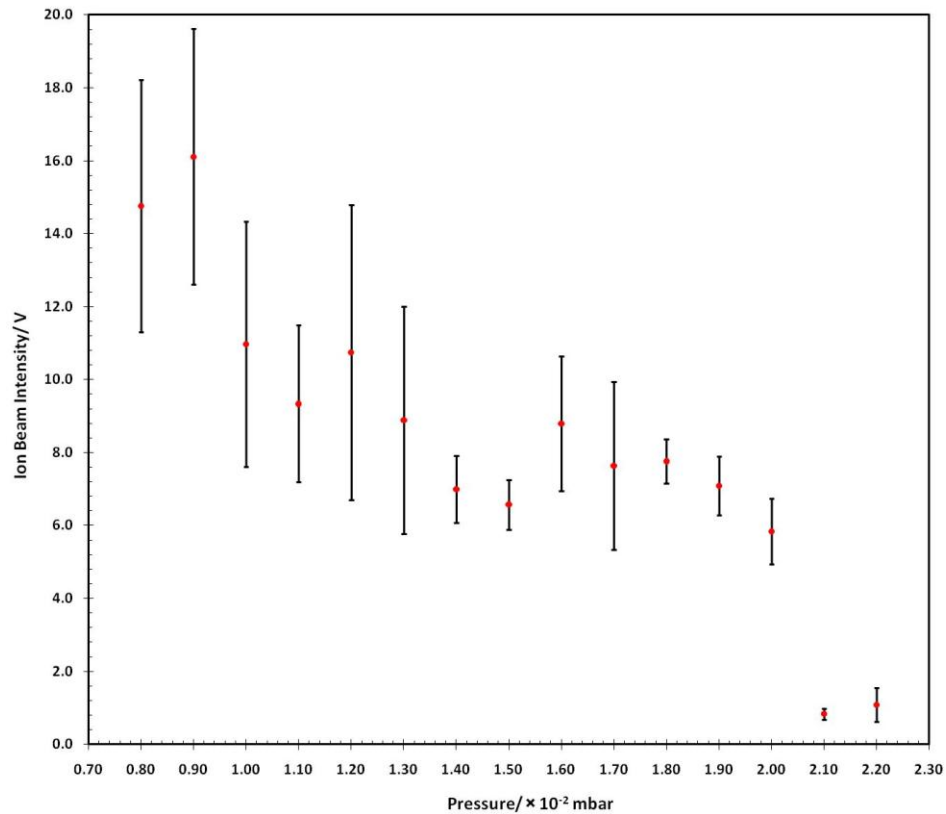


Figure 4.14 Variation of average ion beam intensity of the first peak ion beam pulse in the first biased ion collector at various operating pressures.

Each data point in this figure corresponds to an average of five signals obtained at each operating pressure. The standard deviations are also shown in the graph. The result shows that the ion beam is increased as the pressure is decreased, where higher amplitude peaks are observed.

A careful analysis of the signals obtained by the two biased ion collectors review the TOF information. In Figure 4.13, we found that the second peak of the two detectors correspond to the first pulse of argon beam, emitted at the instant when the voltage spike is registered. The corresponding TOF gives the energy of the ion beam. Time differences in these peaks are the TOF of the argon beam. The TOF method is illustrated in Figure 4.15. In Figure 4.15, the first peak registered in the voltage signal and the two biased ion collector signal at around $2.1 \mu\text{s}$ are shadowed. These signals are believed to be caused by photons emitted during the plasma pinch. The following peaks are clearly separated when registered by the first and second biased ion collectors. These are the collected argon beams. The group of ion beam travels from the plasma pinch to the first biased ion collector in the time of t_{01} . Same group of ion beam is registered by the second biased ion collector after a delay time of t_{12} , which means that the energetic ion beam traveled from the first biased ion collector to the second biased ion collector separated by a distance of S , 70 cm in a time of t_{12} .

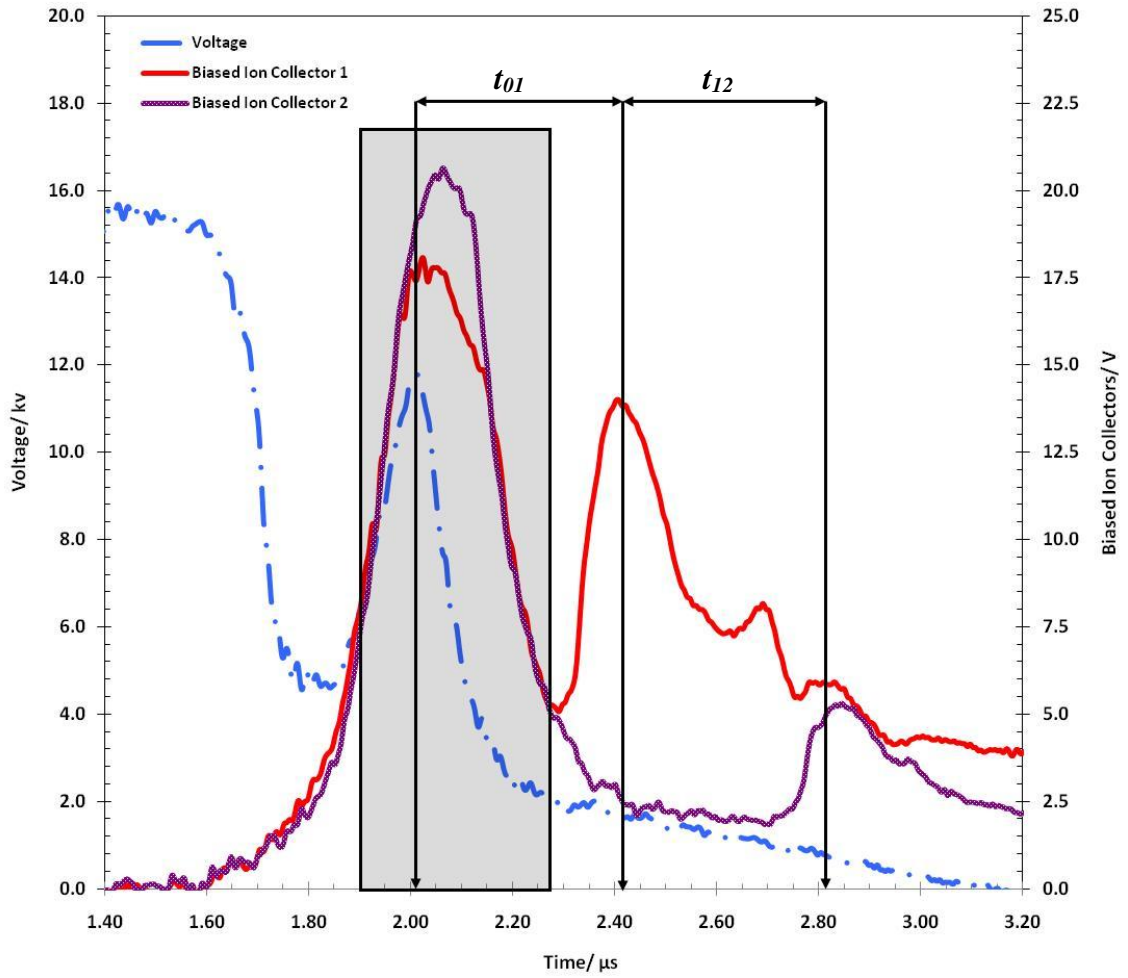


Figure 4.15 The voltage spike and time resolved signals of the ion beam obtained for discharge at 9.0×10^{-3} mbar, 18 kV.

Assuming the peak of ion signal detected to be due to argon ions with each a mass of m and they are traveling together with velocity of v in the vacuum medium. Thus, the ion beam energy can be estimated from the equation

$$E = \frac{1}{2}mv^2 \quad \text{Joules} \quad (4.6)$$

where the velocity of argon ion, v can be expressed as

$$v = \frac{S}{t_{12}} \quad ms^{-1} \quad (4.7)$$

Assuming the dominant peaks correspond to singly charged argon beam, the energy is estimated based on the time of flight information. The calculated argon energies are summarized in Figure 4.16.

The lowest and highest average argon beam energy obtained are 38 keV and 560 keV, respectively. The ion beam energy from the plasma focus is low when the argon pressure is high. The average energy of the argon beam increases with decreasing operating pressure from 2.2×10^{-2} mbar to 9.0×10^{-3} mbar and drops after the pressure of 9.0×10^{-3} mbar. Thus, the pressure of 9.0×10^{-3} mbar argon is concluded to be the best condition for high energy ion beam production for the current setup.

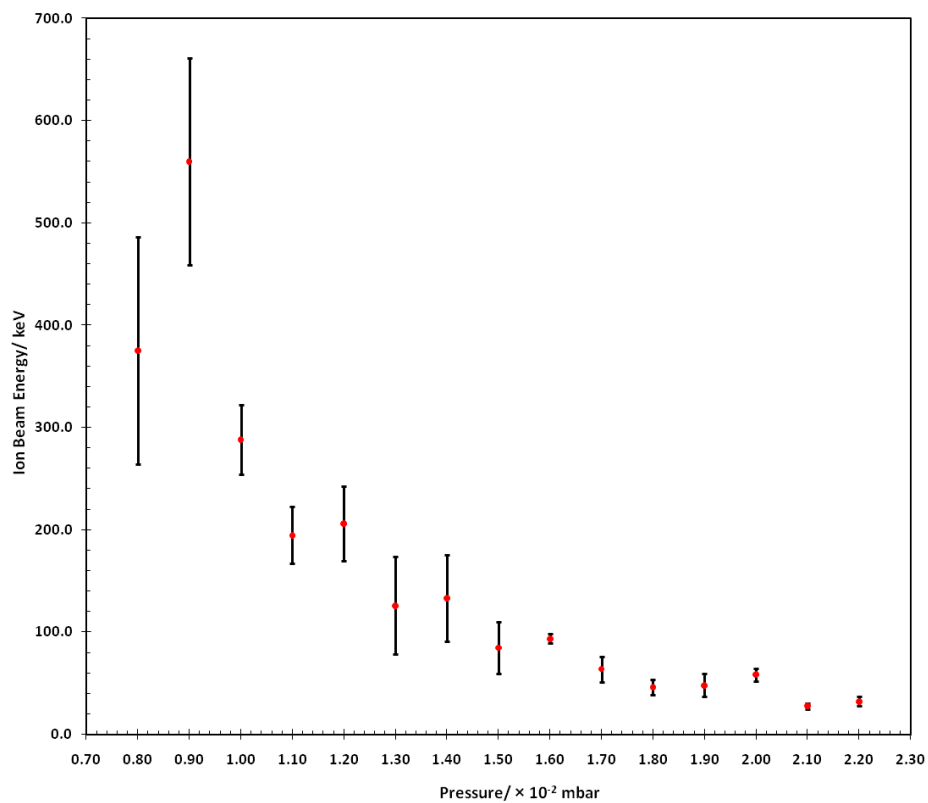


Figure 4.16 Argon beam energy obtained at operating pressures of 8.0×10^{-3} mbar to 2.2×10^{-2} mbar.

In the region where good EUV emissions are obtained, low ion beam emissions are observed. As ion beam emission may contaminate samples for EUV radiation or photodiode which are used for EUV detection especially at the end-on measurement, the condition selected for the production of EUV should be one with low ion beam. In this case, pressures of more than 1.3×10^{-2} mbar are relatively safe. However, to further reduce the possibility of coating due to ion beam, thin filter can be used to block the ion beam but allow EUV to pass through.